

RESEARCH ARTICLE

Open Access



Raloxifene retards the progression of adjacent segmental intervertebral disc degeneration by inhibiting apoptosis of nucleus pulposus in ovariectomized rats

Qi Sun¹, Xin-Yu Nan¹, Fa-Ming Tian², Fang Liu², Shao-Hua Ping¹, Zhuang Zhou³ and Liu Zhang^{1,4*} 

Abstract

Background: Adjacent segmental intervertebral disk degeneration (ASDD) is a major complication secondary to lumbar fusion. Although ASDD pathogenesis remains unclear, the primary cause of intervertebral disk degeneration (IVDD) development is apoptosis of nucleus pulposus (NP). Raloxifene (RAL) could delay ASDD by inhibiting NP apoptosis.

Methods: An ASDD rat model was established by ovariectomy (OVX) and posterolateral spinal fusion (PLF) on levels 4–5 of the lumbar vertebrae. Rats in the treatment groups were administered 1 mg/kg/d RAL by gavage for 12 weeks, following which, all animals were euthanized. Lumbar fusion, apoptosis, ASDD, and vertebrae micro-architecture were evaluated.

Results: RAL maintained intervertebral disk height (DHI), delayed vertebral osteoporosis, reduced histological score, and inhibited apoptosis. The OVX+PLF+RAL group revealed upregulated expression of aggrecan and B-cell lymphoma-2 (bcl2), as well as significantly downregulated expression of a disintegrin and metalloproteinase with thrombospondin motifs 4 (ADAMTS-4), metalloproteinase-13 (MMP-13), caspase-3, BCL2-associated X (bax), and transferase dUTP nick end labeling (TUNEL) staining. Micro-computed tomography (Micro-CT) analysis revealed higher bone volume fraction (BV/TV), bone mineral density (BMD), and trabecular number (Tb.N), and lower trabecular separation (Tb.Sp) in OVX+PLF+RAL group than in the OVX+PLF group.

Conclusions: RAL can postpone ASDD development in OVX rats through inhibiting extracellular matrix metabolic imbalance, NP cell apoptosis, and vertebral osteoporosis. These findings showed RAL as a potential therapeutic target for ASDD.

Keywords: Osteoporosis, Animal, Apoptosis, Intervertebral disk, Fusion

* Correspondence: zhliu130@sohu.com

¹Department of Orthopaedic Surgery, Hebei Medical University, 361 Zhongshan E Rd, Shijiazhuang, Hebei 050000, People's Republic of China
⁴Department of Orthopaedic Surgery, Emergency General Hospital, Beijing, People's Republic of China

Full list of author information is available at the end of the article



© The Author(s). 2021 **Open Access** This article is licensed under a Creative Commons Attribution 4.0 International License, which permits use, sharing, adaptation, distribution and reproduction in any medium or format, as long as you give appropriate credit to the original author(s) and the source, provide a link to the Creative Commons licence, and indicate if changes were made. The images or other third party material in this article are included in the article's Creative Commons licence, unless indicated otherwise in a credit line to the material. If material is not included in the article's Creative Commons licence and your intended use is not permitted by statutory regulation or exceeds the permitted use, you will need to obtain permission directly from the copyright holder. To view a copy of this licence, visit <http://creativecommons.org/licenses/by/4.0/>. The Creative Commons Public Domain Dedication waiver (<http://creativecommons.org/publicdomain/zero/1.0/>) applies to the data made available in this article, unless otherwise stated in a credit line to the data.

Introduction

Lumbar spinal fusion is an effective surgery to treat spinal diseases as it can remove certain lumbar motions [1]. However, it is associated with caudad and cephalad motions near the fusion site, resulting in a high incidence of adjacent segmental intervertebral disk degeneration (ASDD) [2]. ASDD incurs a huge economic and psychological burden on patients and families, seriously affecting the patient's quality of life. Nucleus pulposus (NP) constitutes an important component of the intervertebral disk (IVD). NP can form an integrated IVD with cartilage endplate (EP) and annulus fibrosus (AF). Extracellular matrix (ECM) mostly comprises collagens, proteoglycans, and aggrecan that form the gelatinous tissues within the IVD [3]. The degeneration of NP is an indispensable aspect of intervertebral disk degeneration (IVDD) [4].

Increasing evidence shows that estrogen influences the health of IVDD [5, 6]. The estrogen deficiency after menopause has a negative impact on the vertebral body and endplates, which increases the risk of IVDD in the postmenopausal period [6, 7]. The pathogenesis of ASDD is not completely understood. However, the apoptosis of NP, as well as the changes in the nutritional absorption in IVD are speculated to participate in ASDD development. Although inflammation and apoptosis maintain tissue homeostasis in the body, excessive apoptosis of NP cells accelerates the IVDD [8]. According to Che and colleagues [9], suppression of NP cell apoptosis delayed IVD degeneration.

Raloxifene (RAL), a second-generation, non-steroidal, selective estrogen receptor modulator (SERM), modulates bone turnover and the nervous system. In addition, it affects several metabolic processes, such as apoptosis, inflammation, and aging, by functioning as the estrogen agonist or antagonist [10, 11]. Several studies have reported the protective effects of RAL against chondrocyte apoptosis, senescence, and bone loss [12–14]. Although NP is the primary component of IVD, the regulatory role of RAL in NP has remained largely unclear. As apoptosis significantly affects IVDD, we speculated RAL to be implicated in ASDD pathogenesis.

We used an ovariectomy (OVX) and posterolateral spinal fusion (PLF) rat model to study the effects of RAL on ASDD. Besides, this study examined the mechanisms responsible for the RAL function in ASDD.

Materials and methods

Experimental design

The present study was approved by the Institutional Animal Care and Use Committee. Altogether, 60, 3-month-old Sprague Dawley (SD) rats (Vital River Experimental Animal Technical Co., Ltd., Beijing) weighing 216 ± 14 g (mean \pm SD) were randomized into two

groups, including the sham group (sham surgery, $n = 24$) and OVX group (bilateral ovariectomy, $n = 36$). The animals in the sham surgery group were randomly assigned to the sham group ($n = 12$) and PLF group ($n = 12$). The animals in the OVX group were randomly assigned to the OVX group ($n = 12$), OVX+PLF group ($n = 12$), and OVX+PLF+RAL group ($n = 12$). PLF surgery was performed at L4–L5 using a previously described procedure [15, 16]. The rats in the OVX+PLF+RAL group were administered 1 mg/kg/d RAL by gavage for 12 weeks. All rats were euthanized at 12 weeks post-PLF to collect the L3–L6 segment.

The rats were maintained at 21 ± 1 °C and 12-h light/dark cycle conditions and were provided food and water freely (HFK Bioscience Co., Ltd., Beijing).

Manual palpation and X-ray analysis

The L3–L6 segment fusion was evaluated in the lateral recumbent position by soft radiography (DR7500 System, Kodak, USA). The disk height index (DHI) was determined by this formula: anterior disk height + posterior disk height/anterior vertebral bone height + posterior vertebral bone height. Manual palpation is considered a gold standard for assessing the success of pseudarthrosis formation and fusion [17]. The fusion scores were evaluated according to the criteria established by O'Loughlin et al. [18].

Micro-CT analysis

For investigating changes in vertebrae, the SkyScan 1176 microcomputed tomography system (80 kV, 313 μ A, 18 μ m) was used to scan the L5–L6 segments. One inner cylinder with a diameter and length of 1.5 mm and 3 mm, respectively, was chosen to be the region of interest (ROI) in L6 vertebrae at the cephalad level. To evaluate the vertebral trabecular structural parameters, we determined the bone mineral density (BMD), trabecular number (Tb.N), trabecular separation (Tb.Sp), and bone volume fraction (BV/TV).

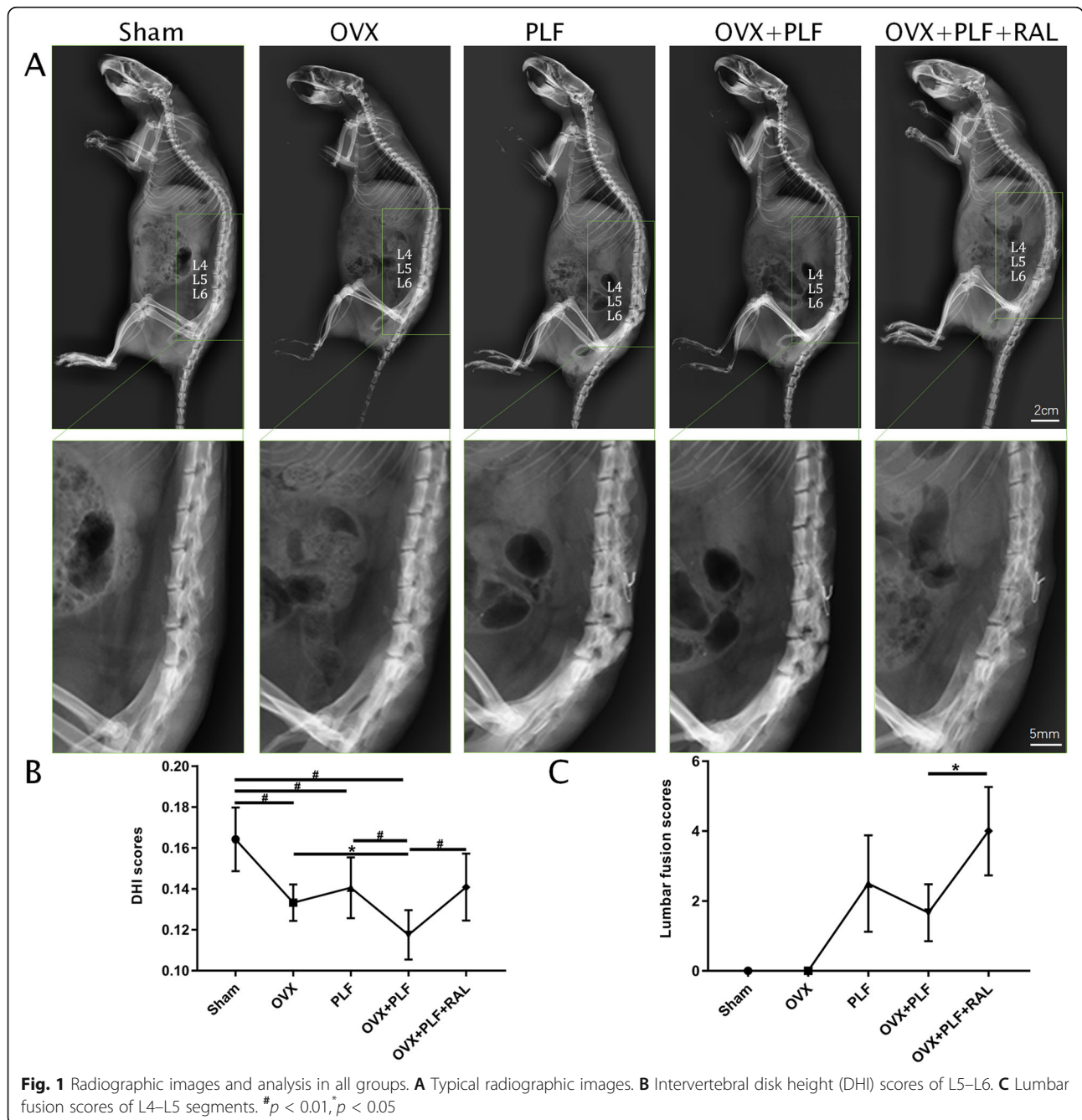
Histology and immunohistochemistry examinations

Neutral paraformaldehyde (10%) was used to fix the specimens for 48 h at room temperature. Ethylenediaminetetraacetic acid (EDTA)-2Na (10%) was used for further decalcification for 3 months. Thereafter, each specimen was dehydrated, paraffinized, and embedded. Next, each sample was cut into 8- μ m sections for terminal deoxynucleotidyl transferase dUTP nick end labeling (TUNEL) staining, Van Gieson (VG) staining, and immunohistochemical (IHC) analysis. VG and TUNEL staining were performed as per the protocols provided with the BA408A VG kit and MA0224 one-step TUNEL apoptosis kit, respectively. The L5–L6 IVD degeneration was studied using histological scoring [19], which was

performed by two independent researchers in a blinded manner.

Expression of caspase 3 (1:100; Gene Tex Inc., USA), ADAMTS-4 (1:100; Abcam Inc, USA), matrix metalloproteinase-13 (MMP-13) (1:500; Boster Co., Ltd., Wuhan, China), aggrecan (1:100; Abcam Inc., USA), BCL2-associated X (bax) (1:200; Abcam Inc., USA), and B cell lymphoma-2 (bcl2) (1:300; Abcam Inc., USA) in NP was detected by IHC. Each section was deparaffinized, rehydrated, and immunostained

in succession, followed by 30 min of incubation by pancreatin to retrieve the antigens at 37 °C. Afterwards, 3% H₂O₂ was used to block endogenous peroxidase activity, and primary antibodies were used to incubate overnight under 4 °C. On the next day, each section was rinsed with Tris-buffered saline for 15 min, followed by further incubation using biotin-labeled goat anti-rabbit IgG (ZSGB-BIO, PV-6000). Later, diaminobenzidine (ZSGB-BIO Corp., China), a chromogenic substrate, was used for color



development, and hematoxylin was used to counter-stain the sections.

The Imaging Pro Plus 6.0 software (Media Cybernetics, Inc., USA) was used to calculate the ROI and to integrate the optical density (IOD). For measuring the mean IOD of certain proteins, we divided the total IOD by ROI, which was reported as IOD/mm².

Statistical analysis

SPSS20.0 (SPSS Inc.; Chicago, IL, USA) was applied in statistical analysis. Values were expressed in as mean ± SD. Normal distribution and homogeneity of variances were evaluated by Shapiro–Wilk and Bartlett’s test. One-way analysis of variance (ANOVA) and Fisher’s protected least significant difference (LSD) test were adopted for analyzing significant differences. Kruskal–Wallis test was applied in analyzing lumbar fusion scores. P < 0.05 suggested that a difference was of statistical significance.

Results

Manual palpation and X-ray analysis

Radiography was performed to observe the effects of DHI and lumbar fusion post-RAL treatment. According to Fig. 1, PLF, OVX, and OVX+PLF groups showed decreased DHI relative to sham group, whereas OVX+PLF+RAL group showed markedly increased DHI as compared with OVX+PLF groups. After manual palpation, there was no detectable movement at the fusion level. In contrast to the OVX+PLF group, those in the OVX+PLF+RAL group had elevated lumbar fusion scores. The difference was not significant in the PLF group relative to the OVX+PLF group.

Histological examinations

To assess the function of RAL, we performed VG staining to observe adjacent segmental intervertebral disk and examine the histological structure. According to Fig. 2, compared with PLF, OVX, and OVX+PLF groups, certain notochord cells surrounded by rich ECM were observed

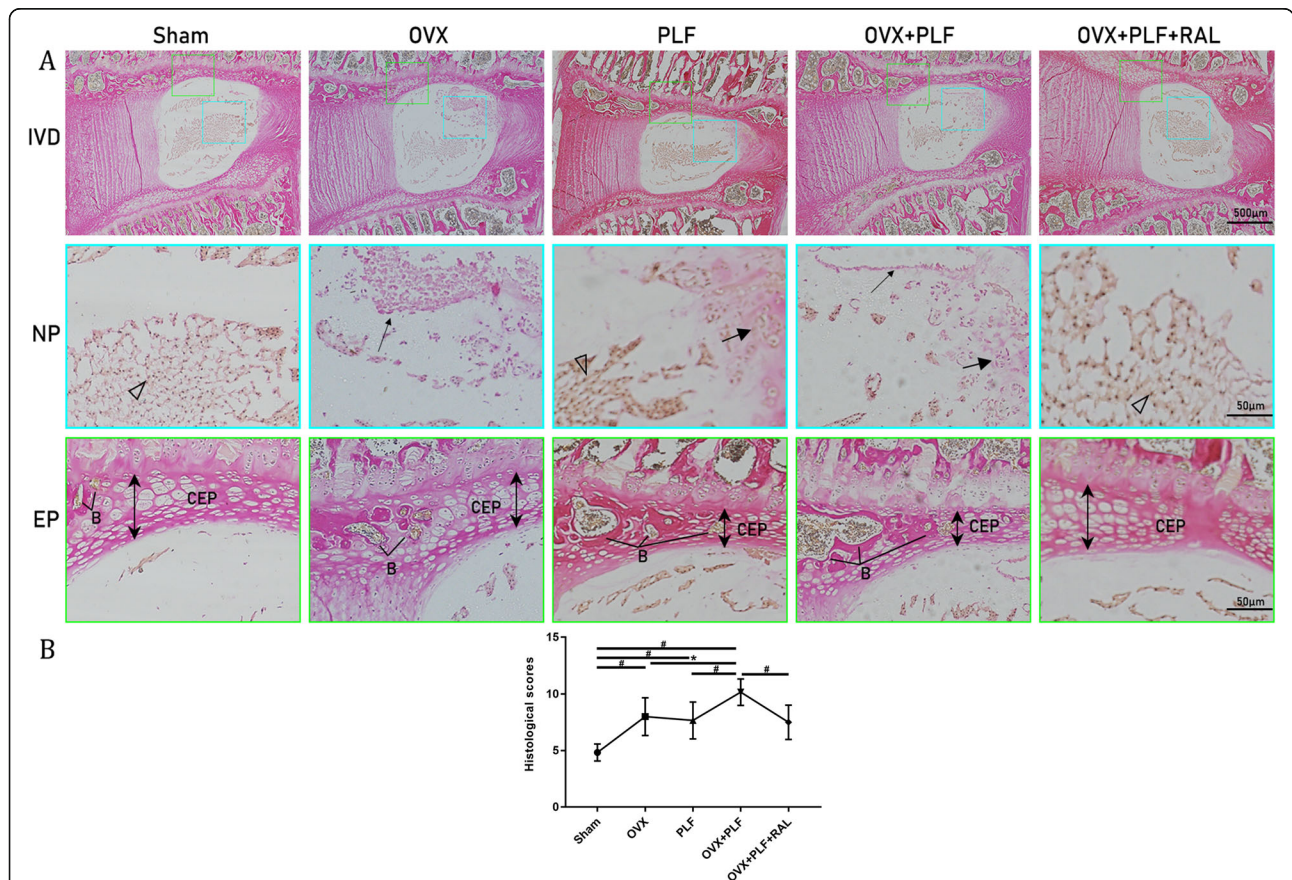
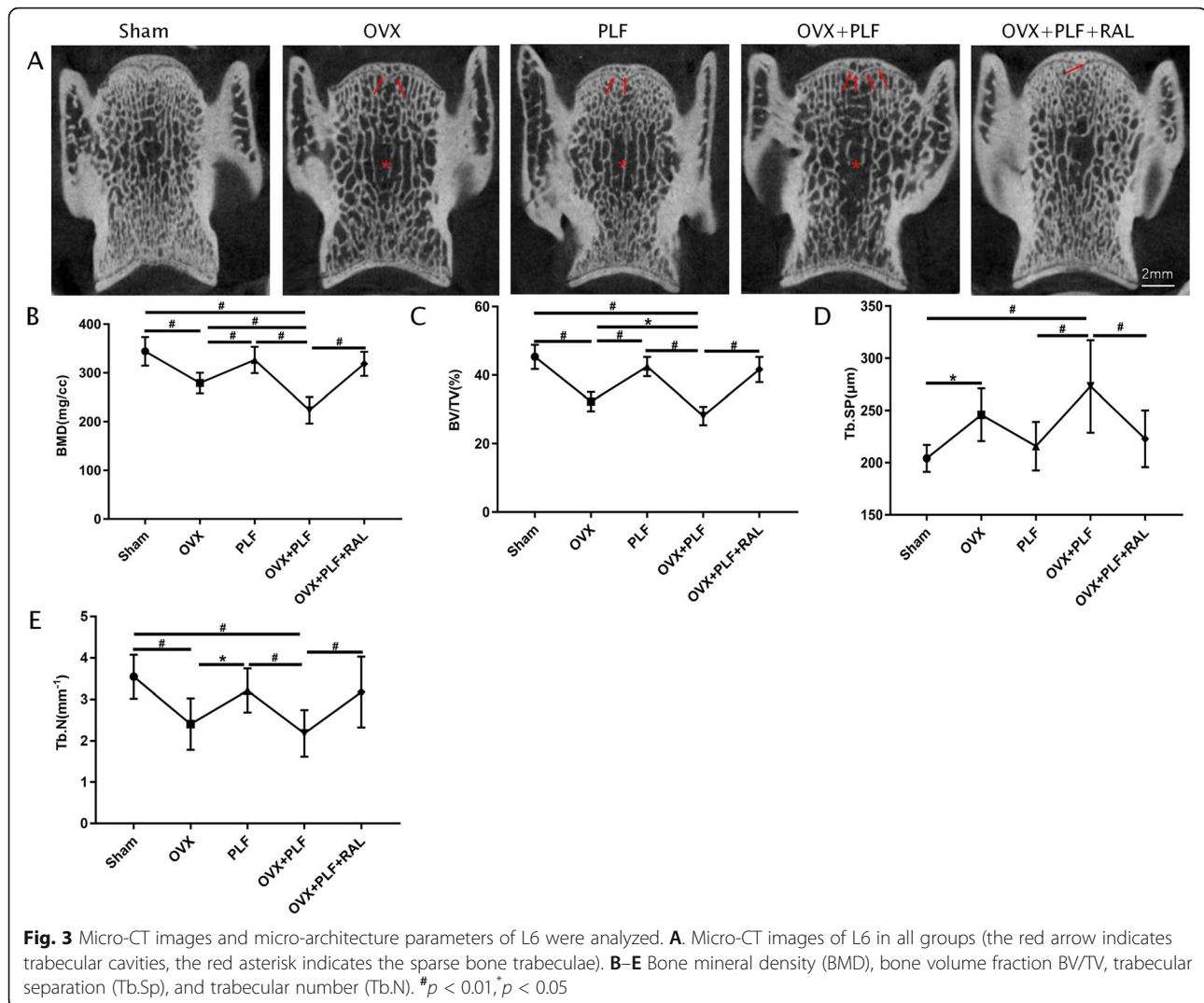


Fig. 2 Van Gieson (VG) staining and histological scores of L5–L6 segments in each group. **A** Intervertebral disk degeneration (IVD), nucleus pulposus (NP) (notochord cells are indicated by the blank arrow, mucoïd degeneration of NP is indicated by the thin arrow, and the doublets of chondrocyte-like cells are indicated by the large arrow), and endplate (EP). The double arrow represents the thickness of EP. CEP, cartilage endplate; VP, vertebral physis; B, bony tissues. **B** Histological scores. #p < 0.01, *p < 0.05



in the sham group. AF was neatly arranged, and chondrocytes were observed within the EP. In addition, certain NP cells in PLF, OVX, and OVX+PLF groups were substituted by chondrocyte-like cell clusters. Mucoïd degeneration to varying degrees was observed in the matrix surrounding the NP cells, with calcification within the EP. Aggravated degeneration was observed in the OVX+PLF group. But RAL treatment efficiently postponed such degenerative changes, as confirmed by histological score results.

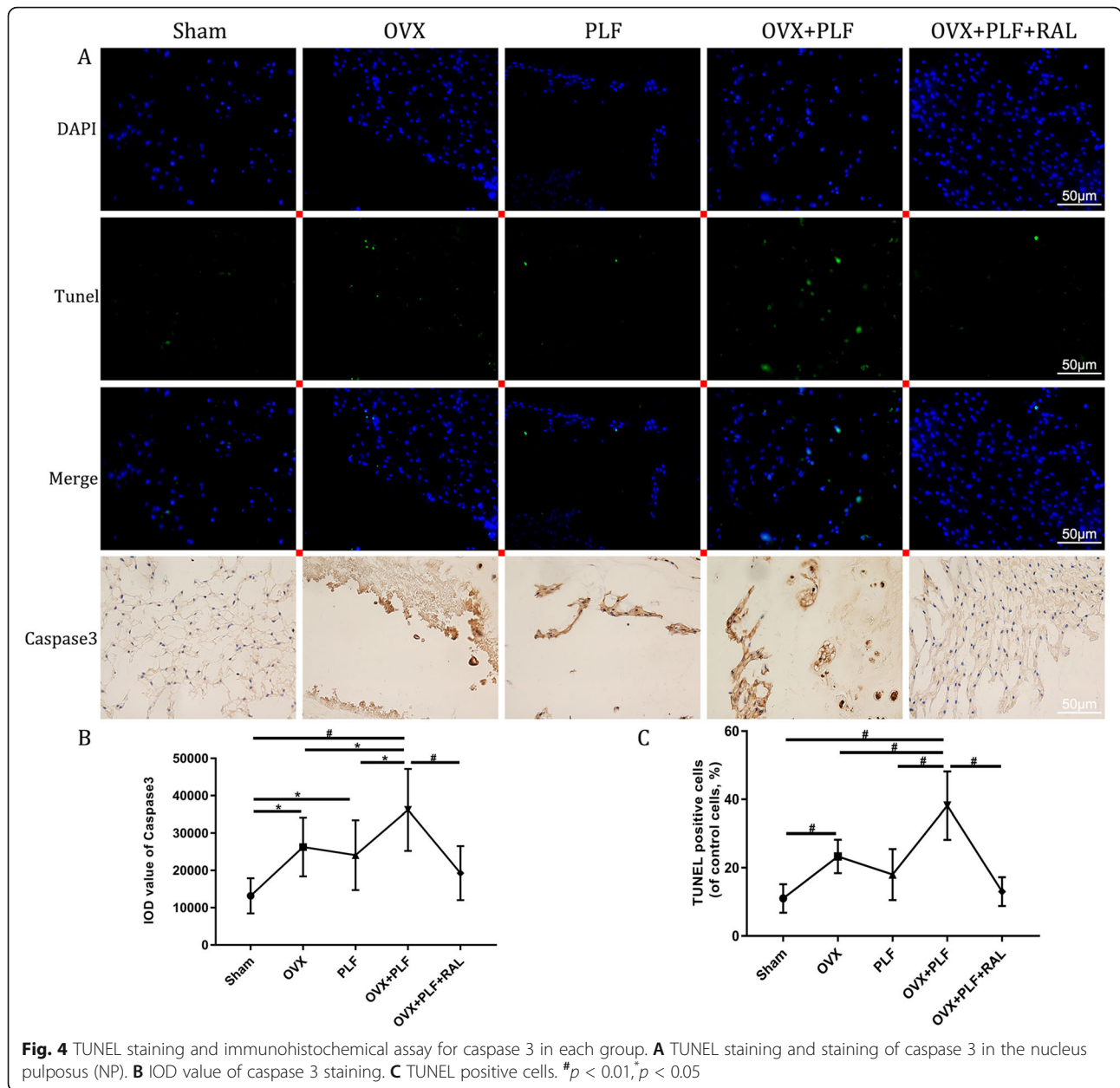
Micro-CT analysis of L6 vertebra

According to Fig. 3, vertebral trabeculae and cavities were largely missing in PLF, OVX, and OVX+PLF groups. The RAL treatment markedly preserved the vertebral architecture. The micro-CT analysis confirmed that rats in the sham group exhibited significantly higher BV/TV, BMD, and Tb.N than those in other groups, but lower Tb.Sp relative to

OVX and OVX+PLF groups. The OVX+PLF groups demonstrated higher BV/TV, BMD, and Tb.N but lower Tb.Sp relative to OVX+PLF+RAL groups. Nonetheless, the difference was not significant in the sham group compared with the PLF group. This confirmed that RAL delayed ASDD by maintaining the structure of the vertebra.

Apoptosis examinations

To evaluate the apoptosis of NP, TUNEL and immunohistochemical staining were performed. Sham group showed markedly increased apoptosis and caspase 3 levels compared with those in the PLF, OVX, and OVX+PLF groups, whereas RAL exposure reduced apoptosis and declined caspase 3 and bax levels but increased bcl2 level relative to the OVX+PLF group (Figs. 4 and 5). These results verified the inhibitory effects of RAL on apoptosis in NP.

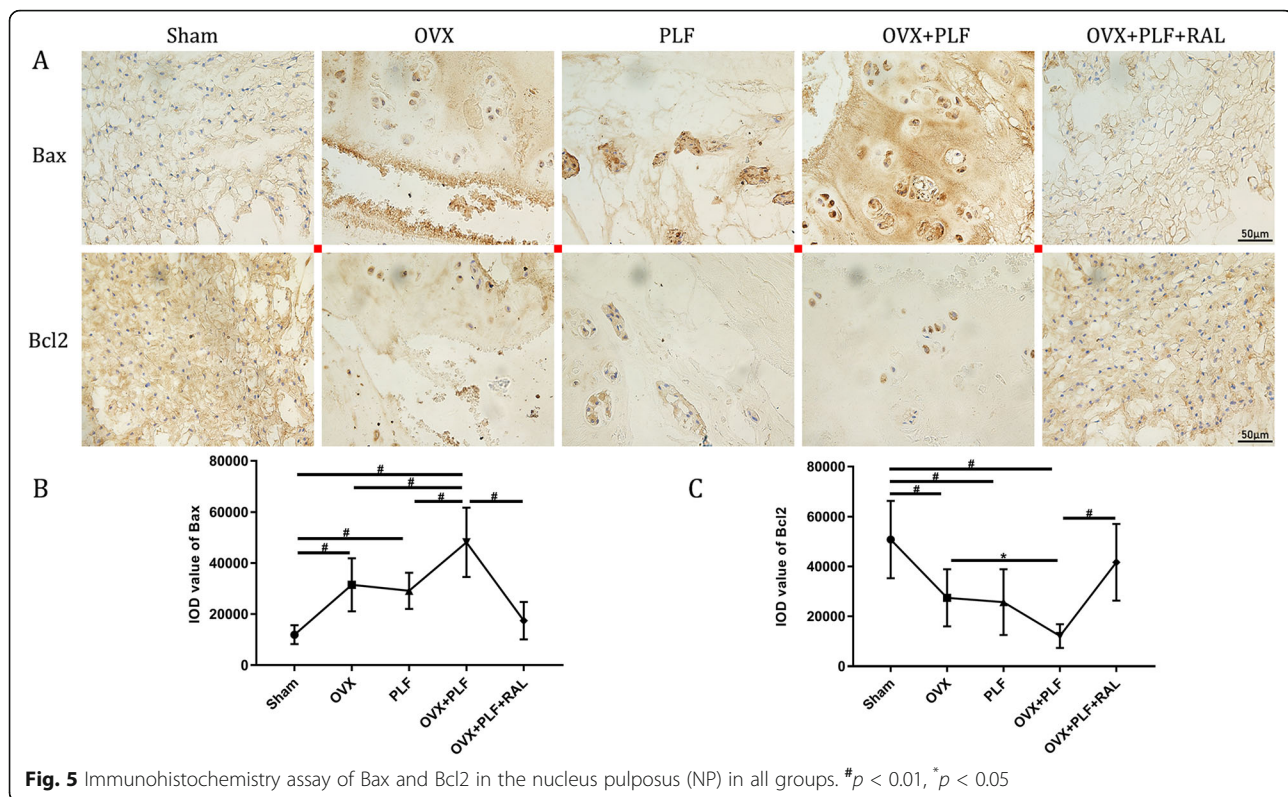


Immunohistochemical assessments

The aggrecan level was markedly reduced in PLF, OVX, and OVX+PLF groups as compared with that in the sham group. However, aggrecan level was elevated in the OVX+PLF+RAL group relative to the OVX+PLF group. MMP-13 and ADAMTS-4 levels markedly elevated in PLF, OVX, and OVX+PLF rats relative to the sham group, but declined in OVX+PLF+RAL groups compared with OVX+PLF group (Fig. 6). These findings verified that RAL protected against ECM in IVD.

Discussion

Although the postoperative effect is unsatisfactory, surgery is the primary alternative for clinical treatment of ASDD. Because ASDD has high morbidity and limited current treatment modalities, studies on finding an effective therapeutic drug and exploring the pathogenesis of ASDD are urgently required. Our study showed that ASDD could be delayed by RAL in ovariectomized rats with lumbar fusion. Radiographic and micro-CT analyses revealed that RAL treatment preserved the vertebral microstructure and DHI. The



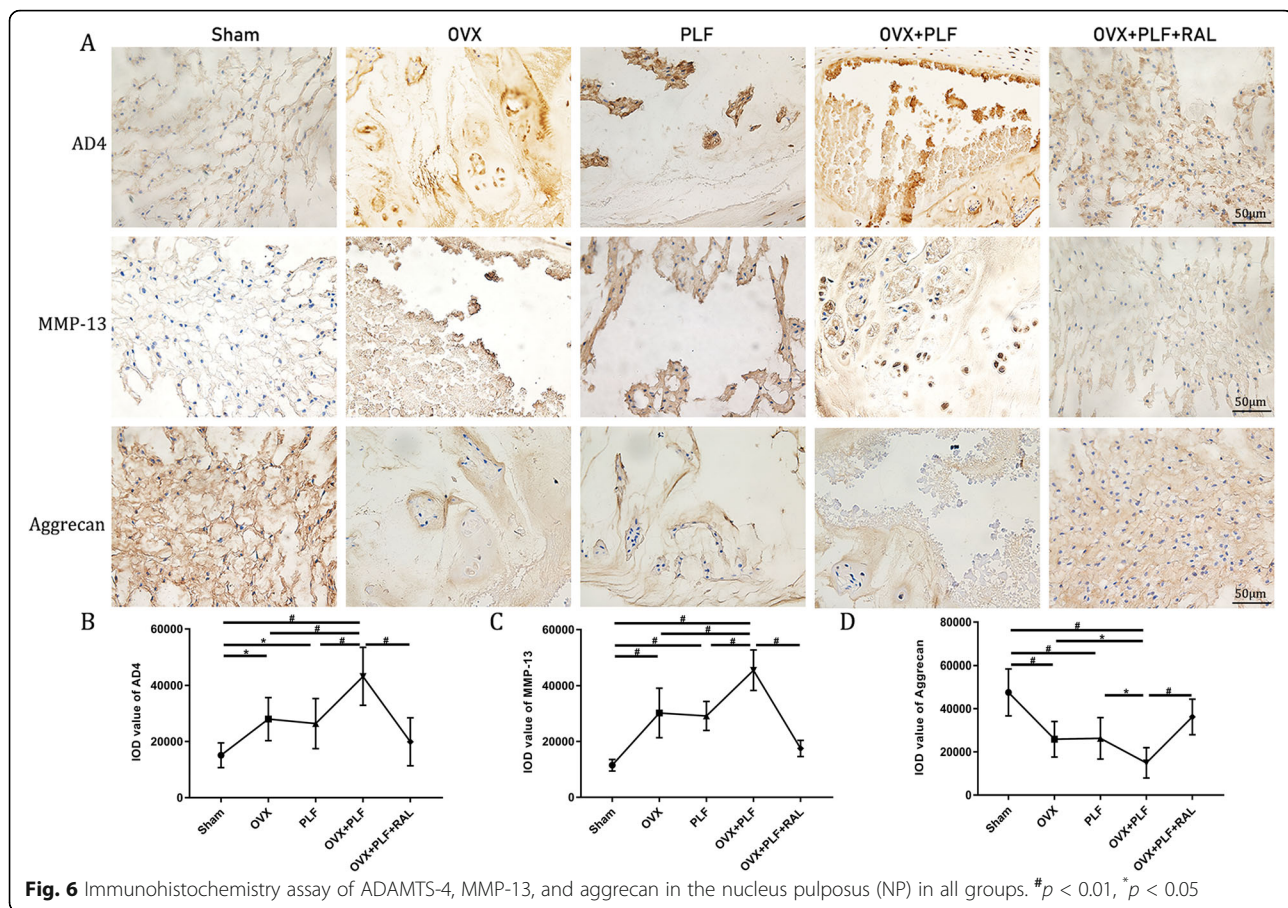
above findings indicated that RAL might be used to treat ASDD.

Osteoporosis is characterized by reduced bone mass, bone microstructure destruction, and high fracture risk, which is more common in postmenopausal women. Some studies have confirmed that osteoporosis caused by estrogen deficiency can accelerate IVDD [20, 21]. For the simulation of this population, we performed OVX surgery to create a model of ASDD with osteoporosis in rats. According to Higashino et al. [22], BMD, DHI, and MRI signal intensity declined at 12 months post-spinal fusion in caudad. In this study, IVDD occurred in the adjacent disks after PLF, which was confirmed by a previous study [23]. In addition, the radiography and micro-CT analysis revealed that estrogen deficiency accelerated the L6 vertebral bone structural deterioration, postponed lumbar fusion, and decreased DHI of the L5–L6 segment. These destructive effects are inhibited by RAL treatment. In addition, the loss and degradation of ECM in the NP is an important pathological feature in IVDD. NP cells mainly synthesize ECM including collagen protein, proteoglycans, and water, which are the main components of the gelatinous tissues of NP [24]. They provide the ability for normal intervertebral disk resistance pressure. ADAMTS-4 is an aggrecan hydrolase, which accelerates the catabolism of aggrecan in the NP and further aggravates the degeneration of the intervertebral disk [25, 26]. MMP-13 can accelerate the degradation of the extracellular matrix, which

plays an important role in IVDD [27]. In this study, we found that RAL could delay ASDD by downregulating the expression of ADAMTS4 and MMP13 but upregulating the expression of aggrecan.

Several studies have reported that estrogen deficiency exacerbates IVD, but estrogen supplementation hinders disk degeneration [28, 29]. Estrogen replacement therapy (ERT) can effectively inhibit the decrease in BMD caused by estrogen deficiency, improve the microstructure of bone trabecula, and reduce the fracture risks [21]. However, the application of ERT increases the risk of pituitary adenomas and reproductive cancers [30]. RAL, a SERM, not only supplements estrogen but also has no adverse effect of ERT [31]. Our results showed that relative to OVX+PLF group, OVX+PLF+RAL group showed elevated Tb.N, BMD, and BV/TV of the L6 segment and DHI. Following RAL treatment, increased osteolysis at the fusion site and increased radiographic density were observed in the L4–L5 segments group relative to the OVX+PLF group.

The generation of inflammatory factors, NP apoptosis, and ECM decomposition has been implicated in ASDD pathogenesis [32]. The apoptosis of NP may accelerate additional degeneration during IVDD [3]. Apoptosis leads to microenvironment transformation, disturbed nutrient absorption, and NP oxidative stress in the IVD, accelerating ASDD [33]. Chen et al. [34] verified the effects of metformin on reversing IVDD by suppressing



NP apoptosis. Our results verified the markedly reduced ADAMT4, MMP-13, caspase 3 and bax levels, and TUNEL-positive cells but increased bcl 2 level among OVX+PLF group following RAL treatment, along with markedly elevated aggrecan levels in NP, suggesting that RAL suppressed NP apoptosis and ECM decomposition during ASDD. In this context, one limitation of the present study is that rat, as a reptile, is different from human being in terms of walking pattern. It is admitted that it cannot simulate the upright walking pattern of human beings, so the effects of human body weight on ASDD cannot be shown precisely. Therefore, a more suitable animal model is to be selected in future studies, thereby better simulating the physiological and pathological changes of human intervertebral disk.

Conclusions

In summary, our study demonstrated that estrogen deficiency deteriorated ASDD condition by destroying the vertebral body structure. In addition, NP apoptosis and ECM degradation accelerated ASDD pathogenesis. RAL administration delayed ASDD progression, primarily by inhibiting vertebral osteoporosis, NP apoptosis, and

ECM decomposition. These results can offer a new therapeutic option to treat ASDD.

Abbreviations

RAL: Raloxifene; BMD: Bone mineral density; ASDD: Adjacent segmental intervertebral disk degeneration; Micro-CT: Microcomputed tomography; IVD: Intervertebral disk; IVDD: Intervertebral disk degeneration; DHL: Disk height index; OVX: Ovariectomy; PLF: Posterolateral lumbar fusion; Agg: Aggrecan; MMP-13: Metalloproteinase-13; ADAMTS-4: A disintegrin and metalloproteinase with thrombospondin motifs 4; bcl-2: B cell lymphoma-2; bax: BCL2-associated X; ROI: Region of interest; BV/TV: Bone volume fraction; Tb.N: Trabecular number; Tb.Sp: Trabecular separation; TUNEL: Transferase dUTP nick end labeling; AF: Annulus fibrosus; EP: Endplates; NP: Nucleus pulposus; VG: Van Gieson; ERT: Estrogen replacement therapy; ECM: Extracellular matrix; ROI: Region of interest; SERM: Selective estrogen receptor modulator

Acknowledgements

No.

Authors' contributions

Liu Zhang designed the study. Qi Sun, Fang Liu, and Zhuang Zhou keep the animal. Qi Sun and Shao-Hua Ping analyzed the data. Fa-Ming Tian and Xin-Yu Nan critically reviewed the data. Qi Sun drafted the manuscript. All authors contributed to interpreting the data and critically revised the manuscript. The authors read and approved the final manuscript. Liu Zhang is the corresponding author.

Funding

This work was supported by National Natural Science Foundation of China (No. 31671235), Youth Natural Science Foundation of China (No. 81702180),

and Natural Science Foundation of Hebei province (No. H2016209176), which are used for purchasing reagents and experimental animals, maintaining laboratory instruments and part of personnel costs.

Availability of data and materials

The datasets used and/or analyzed during the current study are available from the corresponding author on reasonable request.

Declarations

Ethics approval and consent to participate

All animal experiments were approved by the Institutional Animal Care and Use Committee.

Consent for publication

Animal experiment. Not applicable.

Competing interests

The authors have no actual or potential conflict of interests including any financial, personal, or other relationships with other people or organizations that could inappropriately influence, or be perceived to influence, this paper.

Author details

¹Department of Orthopedic Surgery, Hebei Medical University, 361 Zhongshan E Rd, Shijiazhuang, Hebei 050000, People's Republic of China. ²Medical Research Center, North China University of Science and Technology, Tangshan, People's Republic of China. ³Department of Bone and Soft Tissue Oncology, The Third Hospital of Hebei Medical University, Shijiazhuang, People's Republic of China. ⁴Department of Orthopedic Surgery, Emergency General Hospital, Beijing, People's Republic of China.

Received: 30 March 2021 Accepted: 23 May 2021

Published online: 09 June 2021

References

- Son SM, Choi SH, Shin WC, Lee JS. Symptomatic change of Bertolotti's syndrome after long-level lumbar spinal fusion: a case report. *J Orthop Sci*. 2021;26(1):190–5. <https://doi.org/10.1016/j.jos.2018.04.016>.
- Trivedi NN, Wilson SM, Puchi LA, Lebl DR. Evidence-based analysis of adjacent segment degeneration and disease after LIF: a narrative review. *Global Spine J*. 2018;8(1):95–102. <https://doi.org/10.1177/2192568217734876>.
- Cazzanelli P, Wuertz-Kozak K. MicroRNAs in intervertebral disc degeneration, apoptosis, inflammation, and mechanobiology. *Int J Mol Sci*. 2020;21(10).
- Cheng X, Zhang G, Zhang L, Hu Y, Zhang K, Sun X, et al. Mesenchymal stem cells deliver exogenous miR-21 via exosomes to inhibit nucleus pulposus cell apoptosis and reduce intervertebral disc degeneration. *J Cell Mol Med*. 2018;22(1):261–76. <https://doi.org/10.1111/jcmm.13316>.
- Wang YX, Griffith JF. Menopause causes vertebral endplate degeneration and decrease in nutrient diffusion to the intervertebral discs. *Med Hypotheses*. 2011;77(1):18–20. <https://doi.org/10.1016/j.mehy.2011.03.014>.
- Wang YX, Griffith JF. Effect of menopause on lumbar disk degeneration: potential etiology. *Radiology*. 2010;257(2):318–20. <https://doi.org/10.1148/radiol.10100775>.
- Baron YM, Brincat MP, Galea R, Calleja N. Intervertebral disc height in treated and untreated overweight post-menopausal women. *Hum Reprod*. 2005;20(12):3566–70. <https://doi.org/10.1093/humrep/dei251>.
- Liao Z, Luo R, Li G, Song Y, Zhan S, Zhao K, et al. Exosomes from mesenchymal stem cells modulate endoplasmic reticulum stress to protect against nucleus pulposus cell death and ameliorate intervertebral disc degeneration in vivo. *Theranostics*. 2019;9(14):4084–100. <https://doi.org/10.7150/thno.33638>.
- Che H, Li J, Li Y, Ma C, Liu H, Qin JY, et al. p16 deficiency attenuates intervertebral disc degeneration by adjusting oxidative stress and nucleus pulposus cell cycle. *Elife*. 2020;9. <https://doi.org/10.7554/eLife.52570>.
- Veenman L. Raloxifene as treatment for various types of brain injuries and neurodegenerative diseases: a good start. *Int J Mol Sci*. 2020;21(20).
- Koth VS, Salum FG, de Figueiredo MAZ, Cherubini K. Morphological and immunohistochemical features of tooth extraction sites in rats treated with alendronate, raloxifene, or strontium ranelate. *Clin Oral Investig*. 2020;25(5):2705–16. <https://doi.org/10.1007/s00784-020-03585-x>.
- Lu HF, Chou PH, Lin GH, Chou WH, Wang ST, Adikusuma W, et al. Pharmacogenomics study for raloxifene in postmenopausal female with osteoporosis. *Disease Markers*. 2020;2020:8855423.
- Park S, Heo HA, Min JS, Pyo SW. Effect of raloxifene on bone formation around implants in the osteoporotic rat maxilla: histomorphometric and microcomputed tomographic analysis. *Int J Oral Max Impl*. 2020;35(2):249–56.
- Pozios I, Seel NN, Hering NA, Hartmann L, Liu V, Camaj P, et al. Raloxifene inhibits pancreatic adenocarcinoma growth by interfering with ER beta and IL-6/gp130/STAT3 signaling. *Cell Oncol*. 2020;44(1):167–77. <https://doi.org/10.1007/s13402-020-00559-9>.
- Boden SD, Schimandle JH, Hutton WC. An experimental lumbar intertransverse process spinal fusion model. Radiographic, histologic, and biomechanical healing characteristics. *Spine (Phila Pa 1976)*. 1995;20(4):412–20.
- Dimar JR 2nd, Ante WA, Zhang YP, Glassman SD. The effects of nonsteroidal anti-inflammatory drugs on posterior spinal fusions in the rat. *Spine (Phila Pa 1976)*. 1996;21(16):1870–6. <https://doi.org/10.1097/00007632-199608150-00006>.
- DePalma AF, Rothman RH. The nature of pseudarthrosis. *Clin Orthop Relat Res*. 1968;59:113–8.
- O'Loughlin PF, Cunningham ME, Bukata SV, Tomin E, Poynton AR, Doty SB, et al. Parathyroid hormone (1–34) augments spinal fusion, fusion mass volume, and fusion mass quality in a rabbit spinal fusion model. *Spine (Phila Pa 1976)*. 2009;34(2):121–30. <https://doi.org/10.1097/BRS.0b013e318191e687>.
- Mosley GE, Wang M, Nasser P, Lai A, Charen DA, Zhang B, et al. Males and females exhibit distinct relationships between intervertebral disc degeneration and pain in a rat model. *Sci Rep*. 2020;10(1):15120. <https://doi.org/10.1038/s41598-020-72081-9>.
- Chen CH, Chen WC, Lin CY, Chen CH, Tsuang YH, Kuo YJ. Sintered dicalcium pyrophosphate treatment attenuates estrogen deficiency-associated disc degeneration in ovariectomized rats. *Drug Des Devel Ther*. 2018;12:3033–41. <https://doi.org/10.2147/DDDT.S170816>.
- Liu Q, Wang X, Hua Y, Kong G, Wu X, Huang Z, et al. Estrogen deficiency exacerbates intervertebral disc degeneration induced by spinal instability in rats. *Spine (Phila Pa 1976)*. 2019;44(9):E510–9. <https://doi.org/10.1097/BRS.0000000000002904>.
- Higashino K, Hamasaki T, Kim JH, Okada M, Yoon ST, Boden SD, et al. Do the adjacent level intervertebral discs degenerate after a lumbar spinal fusion? An experimental study using a rabbit model. *Spine (Phila Pa 1976)*. 2010;35(22):E1144–52. <https://doi.org/10.1097/BRS.0b013e3181e504d3>.
- Liu CC, Tian FM, Zhou Z, Wang P, Gou Y, Zhang H, et al. Protective effect of calcitonin on lumbar fusion-induced adjacent-segment disc degeneration in ovariectomized rat. *BMC Musculoskelet Disord*. 2015;16(1):342. <https://doi.org/10.1186/s12891-015-0788-7>.
- Wu X, Liu Y, Guo X, Zhou W, Wang L, Shi J, et al. Prolactin inhibits the progression of intervertebral disc degeneration through inactivation of the NF-kappaB pathway in rats. *Cell Death Dis*. 2018;9(2):98. <https://doi.org/10.1038/s41419-017-0151-z>.
- Wang J, Liu X, Sun B, Du W, Zheng Y, Sun Y. Upregulated miR-154 promotes ECM degradation in intervertebral disc degeneration. *J Cell Biochem*. 2019;120(7):11900–7. <https://doi.org/10.1002/jcb.28471>.
- Rogerson FM, Last K, Golub SB, Gauci SJ, Stanton H, Bell KM, et al. ADAMTS-9 in mouse cartilage has aggregase activity that is distinct from ADAMTS-4 and ADAMTS-5. *Int J Mol Sci*. 2019;20(3).
- Li HR, Cui Q, Dong ZY, Zhang JH, Li HQ, Zhao L. Downregulation of miR-27b is involved in loss of type II collagen by directly targeting matrix metalloproteinase 13 (MMP13) in human intervertebral disc degeneration. *Spine (Phila Pa 1976)*. 2016;41(3):E116–23. <https://doi.org/10.1097/BRS.0000000000001139>.
- Song MX, Ma XX, Wang C, Wang Y, Sun C, Xu DR, et al. Protective effect of estrogen receptors (ERalpha/beta) against the intervertebral disc degeneration involves activating CCN5 via the promoter. *Eur Rev Med Pharmacol Sci*. 2021;25(4):1811–20. https://doi.org/10.26355/eurrev_202102_25075.
- Jin LY, Song XX, Li XF. The role of estrogen in intervertebral disc degeneration. *Steroids*. 2020;154:108549. <https://doi.org/10.1016/j.steroids.2019.108549>.
- Chavassieux P, Portero-Muzy N, Roux JP, Garnero P, Chapurlat R. Are biochemical markers of bone turnover representative of bone histomorphometry in 370 postmenopausal women? *J Clin Endocrinol Metab*. 2015;100(12):4662–8. <https://doi.org/10.1210/jc.2015-2957>.
- Recker RR, Mittlak BH, Ni X, Klege JH. Long-term raloxifene for postmenopausal osteoporosis. *Curr Med Res Opin*. 2011;27(9):1755–61. <https://doi.org/10.1185/03007995.2011.606312>.

32. Xiong W, Zhou J, Sun C, Chen Z, Guo X, Huo X, et al. 0.5- to 1-fold intervertebral distraction is a protective factor for adjacent segment degeneration in single-level anterior cervical discectomy and fusion. *Spine (Phila Pa 1976)*. 2020;45(2):96–102.
33. Heyde CE, Tschoeke SK, Hellmuth M, Hostmann A, Ertel W, Oberholzer A. Trauma induces apoptosis in human thoracolumbar intervertebral discs. *BMC Clin Pathol*. 2006;6(1):5. <https://doi.org/10.1186/1472-6890-6-5>.
34. Chen D, Xia D, Pan Z, Xu D, Zhou Y, Wu Y, et al. Metformin protects against apoptosis and senescence in nucleus pulposus cells and ameliorates disc degeneration in vivo. *Cell Death Dis*. 2016;7(10):e2441. <https://doi.org/10.1038/cddis.2016.334>.

Publisher's Note

Springer Nature remains neutral with regard to jurisdictional claims in published maps and institutional affiliations.

Ready to submit your research? Choose BMC and benefit from:

- fast, convenient online submission
- thorough peer review by experienced researchers in your field
- rapid publication on acceptance
- support for research data, including large and complex data types
- gold Open Access which fosters wider collaboration and increased citations
- maximum visibility for your research: over 100M website views per year

At BMC, research is always in progress.

Learn more biomedcentral.com/submissions

